Annals of DAAAM for 2012 & Proceedings of the 23rd International DAAAM Symposium, Volume 23, No.1, ISSN 2304-1382
ISBN 978-3-901509-91-9, CDROM version, Ed. B. Katalinic, Published by DAAAM International, Vienna, Austria, EU, 2012
Make Harmony between Technology and Nature, and Your Mind will Fly Free as a Bird
Annals & Proceedings of DAAAM International 2012

FRICTION INFLUENCE ON THE IMPLEMENTATION OF THE UPPER BOUND THEOREM IN INDENTATION PROCESS

BERMUDO GAMBOA, C[arolina]; MARTIN, F[rancisco] & SEVILLA, L[orenzo]

Abstract: *This work proposes, from the methodological point of view, the application of the Upper Bound Theorem (UBT) to indentation processes, in his development of Triangular Rigid Blocks (TRB), using the Modular distribution. With two approaches of different kind of friction, Tresca (m) and Coulomb (μ) friction, different hodographs are present, corresponding to a kinematically admissible velocity field, and studying the influence in its both way. Applying the UBT with TRB for each modular disposition, considering the appropriate distribution and making these differences between the two types of friction, are achieved results consistent with those obtained in other plastic forming processes, both stationary and non-stationary. Finally it is shown the advantage of lower computational cost that offers this method of calculation as well as having identified at any time the physical evolution of the problem.*

Keywords: *upper bound theorem, triangular rigid blocks, indentation, friction*

1. INTRODUCTION

Customarily in the industry, and especially in plastic deformation, it's not necessary the knowledge of the exact value of the minimum energy required to obtain such deformation process. This paper develops the Upper Bound Theorem (UBT), which provides the energy value that guarantees the deformation of the workpiece. The Theorem is especially interesting because, despite it doesn`t provide the exact amount of energy required, it does provide the minimum value at which it is ensured the piece will begin its plastic deformation. The method is especially applicable due to the simplicity, compared with other methods, in case of plane strain.

This study of the necessary energy for the plastic deformation has been tackled traditionally by means of mathematical approaches of different nature, numerical and analytical methods. The inherent complexity of the plasticity theory [1] has conditioned the development of these last quoted methods. The UBT by means of his kinematic-geometrical application has made possible an analytical implementation of limited complexity with which obtain different parameters of calculation related with the deformation in plastic state of the studied part. The result obtained by applying this method is, therefore, approximately, but provides a simple resolution and a significant qualitative approach to solve the problem.

The kinematic-geometrical option is known like the model of Triangular Rigid Blocks that allows reaching precise solutions, with high capacity of analysis, of the main factors that is involve in a process of plastic deformation, applied initially in suppositions of plane strain.

Triangular Rigid Blocks (TRB) are used to develop this thecnique. This model assumes that the stresses and strains that cause deformation in the material, are produced only in the planes which delimits each TRB, because is along these planes where exist speed discontinuity. The other points that conforms the TRB move at the same speed and in the same direction.

Of a theoretical point of view, and under general conditions, the UBT expresses that: *The work realised by the superficial strengths of traction (or compression) real on a rigid body perfect-plastic is lower or the same that the realised by the superficial strengths of traction (or compression) corresponding to any another field of admissible kinematic speeds.*

In the supposition of plane deformation and knowing that the part represent by rigid blocks of material moves ones in others along the discontinuity lines of the speed field, the general expression of this work can express:

$$\int_{S_V} T_i v_i dS_V \leq \int_{S_D^*} k[v^*] dS_D^* + \int_{S_F} T_i v_i^* dS_F \qquad (1)$$

Being:

T_i : External strengths applied on the part to deform.

v_i :Real field of speeds.

S_v : Surfaces of application of the external loads.

k : Shear yield stress.

v^*_i: Field of virtual kinematic admissible speeds.

v^*: Velocity discontinuities.

S^*_D: Discontinuity surfaces.

S_F: External surfaces exposed to external surface stresses

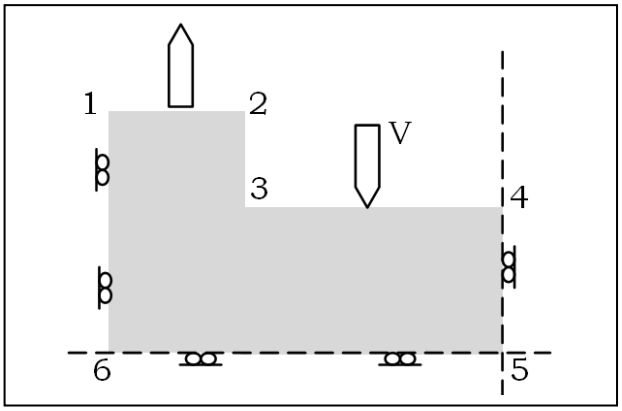

Fig. 1. Boundary conditions indentation process

With plane strain conditions the material offers his maximum resistance to the deformation when $\tau=k$, being τ the shear stress. Thus, the value of the dissipate power because of the internal energy can´t exceed of the value $k \bullet s \bullet v^*$, being s the length of discontinuity line of the tangential speed.

Due to the double symmetry imposed, the study zone turns into a fourth part of the total piece subjected to deformation as shown in Fig. 1 [12].

2. METHODOLOGY

The present work applies the Upper Bound Theorem to indentation processes. In this case, the process is similar to a plane strain under certain geometric conditions, so it allows the analytical treatment by UBT. Implementing the TRB model, are different approaches to the establishment of the satisfactory geometric configuration, as well as its mathematical treatment, being the Modular distribution (Fig. 2) the one that is addressed in this analysis [2, 3, 5]. However, in results section will be offered a compare,son of the Modular model against the Non Modular model (Fig. 3) under the same boundary conditions and shape.

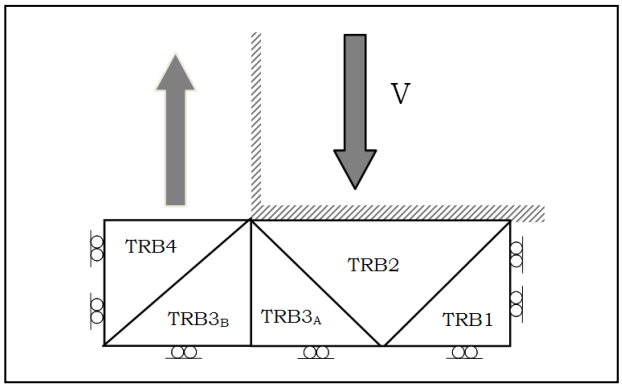

Fig. 2. Modular configuration

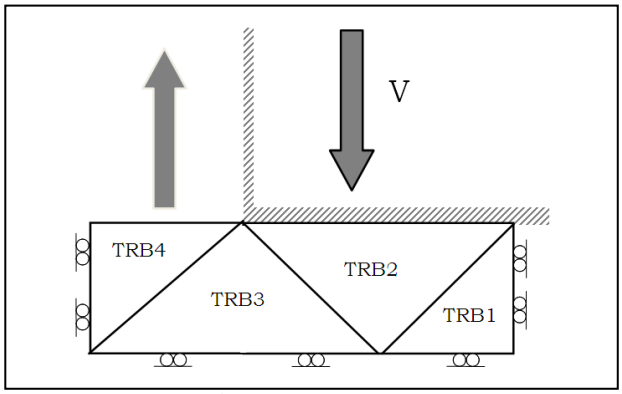

Fig. 3. Non Modular configuration

Modular model consists in the introduction of modules conformed of no more than three TRB, making the connection through the relation between the output and input material speed of each module, as this must be equal in magnitude. To simplify this relationship in the formulation, we allow the same number to the contiguous triangles of different modules, differentiating by adding by subscripts the letter of the module to which it belongs, as shown later in calculations.

Analyzing independently each module and taking into account the relations mentioned, are made different hodographs corresponding to a kinematically admissible velocity field, studying the influence of the incorporation of friction in its two kinds: Tresca (m) and Coulomb friction (μ).

At first we have Module A (Fig. 4, 5), which corresponds to the material located on the horizontal part of the punch, and wich can be divided as follows:

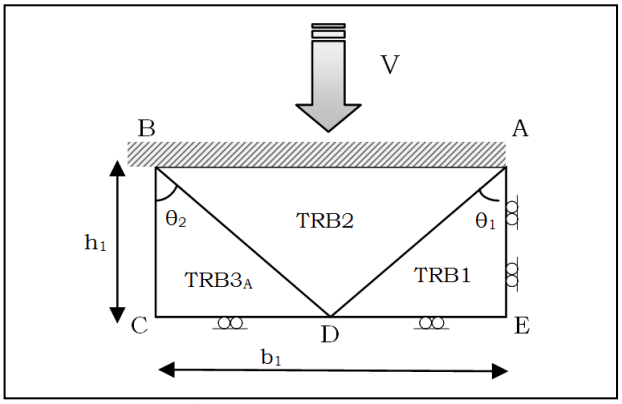

Fig. 4. Module A configuration

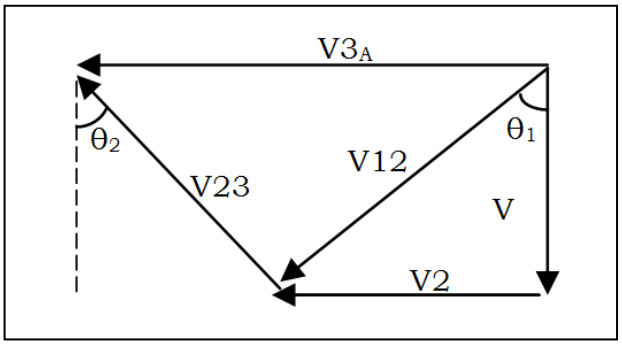

Fig. 5. Module A hodograph

The corresponding equations are as follows, where m and μ are the different kind friction:

Tresca friction (m):

$$p \cdot b_1 \cdot V \cdot w = k \cdot w \cdot [V_1 \cdot ED + V_{12} \cdot AD + V_2 \cdot AB \cdot m + V_{23} \cdot DB + V_{3A} \cdot DC] \quad (2)$$

Coulomb friction (μ):

$$p \cdot b\_1 \cdot V \cdot w = w \cdot [k \cdot [V\_1 \cdot ED + V\_12 \cdot AD + V\_23 \cdot DB + V\_3A \cdot DC] + \mu P \cdot V\_2 \cdot AB] \quad (3)$$

Obtaining the adimensional $p/2k$ relations:

Tresca friction (m):

$$\left(\frac{p}{2k}\right)_A = \frac{1}{2b_1}\left[\frac{2h_1 + {b_1^2}/{2}}{h_1} + \frac{b_1^2 m}{2h_1}\right] \quad (4)$$

Coulomb friction (μ):

$$\left(\frac{p}{2k}\right)_A = \frac{\left(\frac{2h_1^2 + b_1^2/2}{h_1}\right)}{2\left(b_1 - \mu\frac{b_1^2}{2h_1}\right)} \quad (5)$$

From these relations we obtain the results for Module A exposed on Tab. 1

SF	b1	h1	p/2k m=0	p/2k m=1	p/2k μ=0	p/2k μ=0,3
1,00	1	1	1,25	1,50	1,25	1,47
1,05	1	0,95	1,21	1,48	1,21	1,44
1,11	1	0,90	1,18	1,46	1,18	1,41
1,18	1	0,85	1,14	1,44	1,14	1,39
1,25	1	0,80	1,11	1,43	1,11	1,37
1,33	1	0,75	1,08	1,42	1,08	1,35
1,43	1	0,70	1,06	1,41	1,06	1,35
1,54	1	0,65	1,03	1,42	1,03	1,35
1,67	1	0,60	1,02	1,43	1,02	1,36
1,82	1	0,55	1,005	1,46	1,00	1,38
2,00	1	0,50	1,000	1,50	1,00	1,43
2,22	1	0,45	1,01	1,56	1,01	1,51
2,50	1	0,40	1,03	1,65	1,03	1,64
2,86	1	0,35	1,06	1,78	1,06	1,86
3,33	1	0,30	1,13	1,97	1,13	2,27
4,00	1	0,25	1,25	2,25	1,25	3,13
5,00	1	0,20	1,45	2,70	1,45	5,80

Tab. 1. Module A, p/2k results

Knowing that the shape factor value for this module goes from 1 to 5, being the base equal to 1 (b = 1) and modifying the height (h) from 1 to 0,20

On the particular case of indentation, has been created a special module with only two TRB (Fig. 6), unlike the case of forging [7]. This makes a better adaptation to the material elbow relative to the change of direction ($TRB3_B$ and 4, Fig. 2) and ensure an appropriate continuity in all modules, e.g., doesn't create a module with different boundary conditions in each TRB.

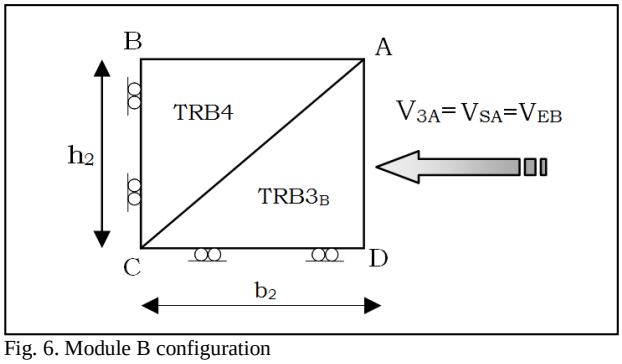

Fig. 6. Module B configuration

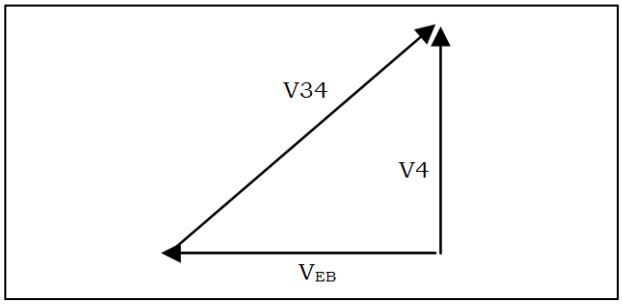

Fig. 7. Hodograph Module B

Further, the hodograph configutarion (Fig. 7) is relatively simple compared to the previous one (Fig. 5).

Just as in the previous module, the corresponding equations are:

Tresca and Coulomb friction:

$$p \cdot b_2 \cdot V \cdot w = k \cdot w \cdot [V_{3B} \cdot CD + V_{4B} \cdot CB + V_{34} \cdot AC] \quad (6)$$

Solving to obtaining the p/*2k* relations:

Tresca and Coulomb friction:

$$\left(\frac{p}{2k}\right)_B = \frac{1}{2b_2}\left[\frac{b_1 h_1}{b_2} + \frac{b_1(h_1^2 + b_2^2)}{h_1 b_2}\right] \quad (7)$$

The equations for the different type of friction coincide in this module because none of its TRB are in contact with the punch.

And from this equation, is obtained the results for Module B exposed on Tab. 2.

SF	b2	h2	p/2k m=0	p/2k m=1	p/2k μ=0	p/2k μ=0,3
1,00	1	1	1,50	1,50	1,50	1,50
1,05	1	0,95	1,48	1,48	1,48	1,48
1,11	1	0,90	1,46	1,46	1,46	1,46
1,18	1	0,85	1,44	1,44	1,44	1,44
1,25	1	0,80	1,43	1,43	1,43	1,43
1,33	1	0,75	1,42	1,42	1,42	1,42
1,43	1	0,70	1,41	1,41	1,41	1,41
1,54	1	0,65	1,42	1,42	1,42	1,42
1,67	1	0,60	1,43	1,43	1,43	1,43
1,82	1	0,55	1,46	1,46	1,46	1,46
2,00	1	0,50	1,50	1,50	1,50	1,50
2,22	1	0,45	1,56	1,56	1,56	1,56
2,50	1	0,40	1,65	1,65	1,65	1,65
2,86	1	0,35	1,78	1,78	1,78	1,78
3,33	1	0,30	1,97	1,97	1,97	1,97
4,00	1	0,25	2,25	2,25	2,25	2,25
5,00	1	0,20	2,70	2,70	2,70	2,70

Tab. 2: Module B, p/2k results

Knowing that the shape factor value goes from 1 to 5, being the base equal to 1 (b = *1*) and modifying the height (h) from 1 to 0,20.

As explained, the results obtained are the same for m and μ for its differents value because this module is not in contact with the punch, so the equation doesn't have friction factors.

The calculation of the ratio *p/2k* combining the influence of both modules ($p_{A+B}/2k$) is determined by equation. 8, where some weight factors are included considering the geometry of each module by means of the width.

$$\frac{p}{2k} = \frac{\left(\frac{p}{2k}\right)_A b_1 + \left(\frac{p}{2k}\right)_B b_2}{(b_1 + b_2)} \quad (8)$$

Analycing now the Non Modular model to a better understanding of the process, in Fig. 8 can be seen that the configuration of the material is similar to the Modular one, i.e. the bases and hight distribution are the same, and have to be the same to maintain an analysis parallel to the Modular configuration and make comparisons with the same shape factors easily.

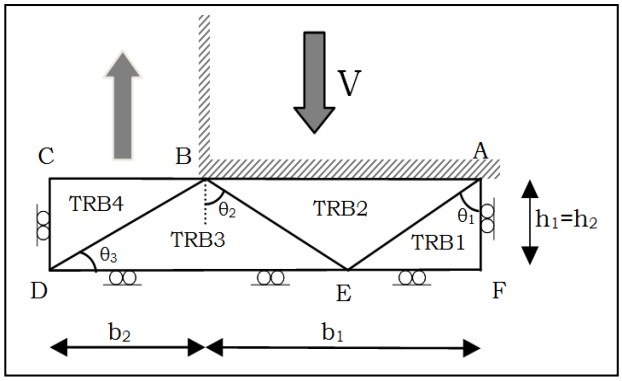

Fig. 8. Non Modular analysis.

As shown in Fig. 9, the hodograph appropriate to the Non Modular model is like a combination of the two hodographs of the Modular model, due to the analogous way of analyze the two models. This helps to ensure the discontinuity lines of the speed field are the same, because if the hodographs are very different it would mean that the speed fields aren't akin and, therefore the comparison would not be suitable.

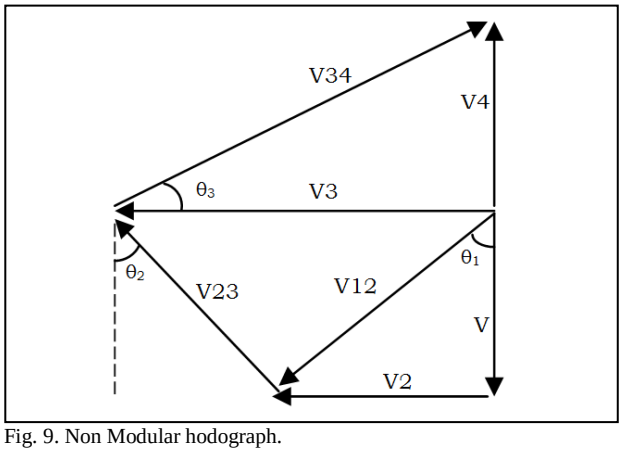

Fig. 9. Non Modular hodograph.

Thus, knowing the configuration and the hodograph, the corresponding equation can be proposed:

Tresca friction (m):

$$p \cdot b \cdot V \cdot w = w \cdot [k \cdot (V_1 \cdot FE + V_{12} \cdot AE + V_{23} \cdot EB + V_3 \cdot ED + V_{34} \cdot BD + V_4 \cdot DC) + V_2 \cdot \mu p \cdot AB] \quad (9)$$

Coulomb friction (μ):

$$p \cdot b \cdot V \cdot w = k \cdot w \cdot [V_1 \cdot FE + V_{12} \cdot AE + V_2 \cdot m \cdot AB + V_{23} \cdot EB + V_3 \cdot ED + V_{34} \cdot BD + V_4 \cdot DC] \quad (10)$$

Being $b = b_1 + b_2$, equation 9 and 10 can be solved:

Tresca friction (m):

$$\frac{p}{2k} = \frac{1}{2b}\left[\frac{2h_1 + b_1^2/2}{h_1} + \frac{b_1^2 m}{2h_1} + \frac{b_1}{h_1}\left(\frac{b_1}{2} + b_2\right) + \frac{b_1(b_2^2 + h_1^2)}{b_2 h_1} + \frac{b_1 h_1}{b_2}\right] \quad (11)$$

Coulomb friction (μ):

$$\frac{p}{2k} = \frac{\frac{2h_1 + b_1^2/2}{h_1} + \frac{b_1}{h_1}\left(\frac{b_1}{2} + b_2\right) + \frac{b_1(b_2^2 + h_1^2)}{b_2 h_1} + \frac{b_1 h_1}{b_2}}{2\left(b - \mu\frac{b_1^2}{2h_1}\right)} \quad (12)$$

And from these equations are obtained the results for Non Modular model exposed in Tab. 3.

SF	b	h2	p/2k m=0	p/2k m=1	p/2k μ=0	p/2k μ=0,3
2,00	2	1	1,38	1,50	1,38	1,49
2,11	2	0,95	1,34	1,48	1,34	1,46
2,22	2	0,90	1,32	1,46	1,32	1,44
2,35	2	0,85	1,29	1,44	1,29	1,42
2,50	2	0,80	1,27	1,43	1,27	1,40
2,67	2	0,75	1,25	1,42	1,25	1,39
2,86	2	0,70	1,24	1,41	1,24	1,38
3,08	2	0,65	1,23	1,42	1,23	1,39
3,33	2	0,60	1,23	1,43	1,23	1,40
3,64	2	0,55	1,23	1,46	1,23	1,43
4,00	2	0,50	1,25	1,50	1,25	1,47
4,44	2	0,45	1,28	1,56	1,28	1,54
5,00	2	0,40	1,34	1,65	1,34	1,65
5,71	2	0,35	1,42	1,78	1,42	1,81
6,67	2	0,30	1,55	1,97	1,55	2,07
8,00	2	0,25	1,75	2,25	1,75	2,50
10,00	2	0,20	2,08	2,70	2,08	3,32

Tab. 3. Non Modular p/2k results

3. RESULTS AND DISCUSSION

It has been made a comparison with a Non Modular model to check out the efficiency of the Modular model. The application of the UBT by TRB has been applied to each model shown in the graphs (Fig. 10 to Fig. 11) for extreme values of friction, both Tresca and Coulomb friction. Because of the type of compression process, it was decided to raise the maximum Coulomb value as 0,3, since higher values do not assimilate the real problem due to the Tresca friction contribution that would be wider.

Results obtained are consistent, at all time, with those obtained in other plastic deformation processes [7], [10], both stationary and non-stationary, been the behavior of both models very similar for the shape factor studied and submitted.

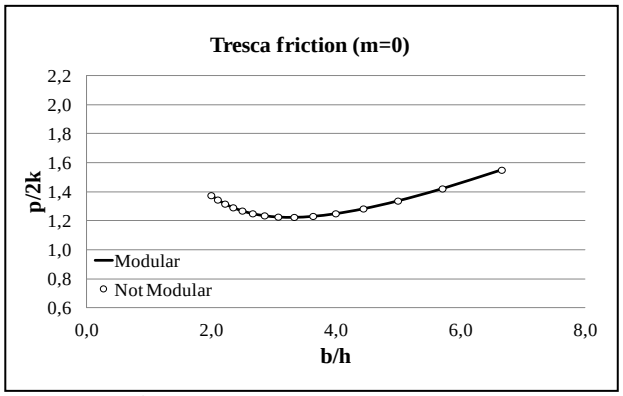

Fig. 10. Tresca friction comparative minimum value

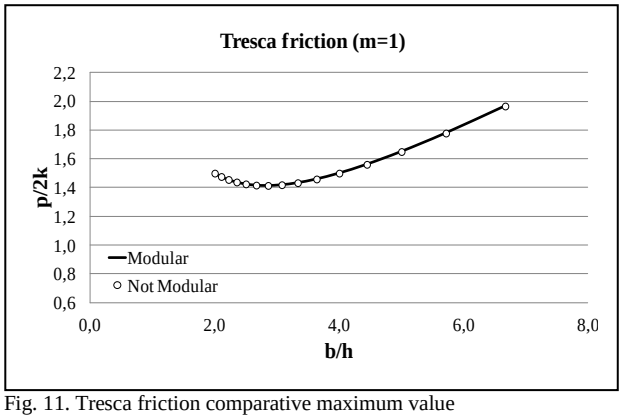

Fig. 11. Tresca friction comparative maximum value

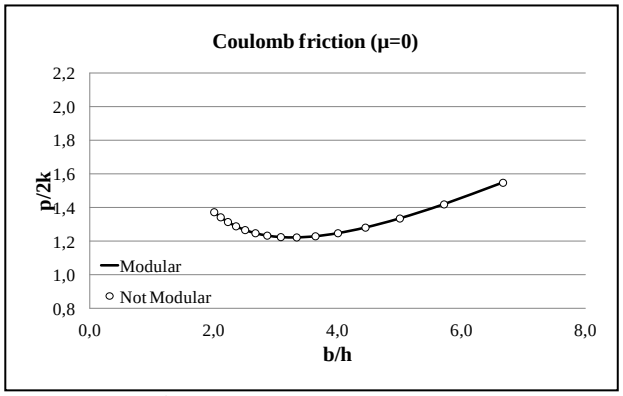

Fig. 12. Coulomb friction comparative minimum value

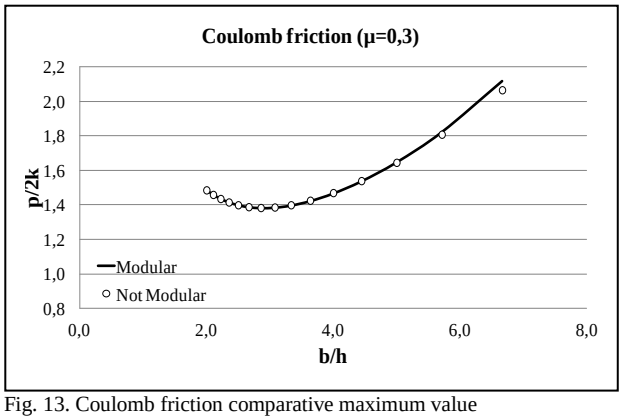

Fig. 13. Coulomb friction comparative maximum value

Its evolutions shows, for both type of friction, the characteristic shape of load curves [4], [5] for different moments of the process, with the appearance of minimum values of the adimensional ratio *p/2k* (where p is the pressure and *k* the yield limit by shear strain. Fig. 14 shows four moments of the deformation process.

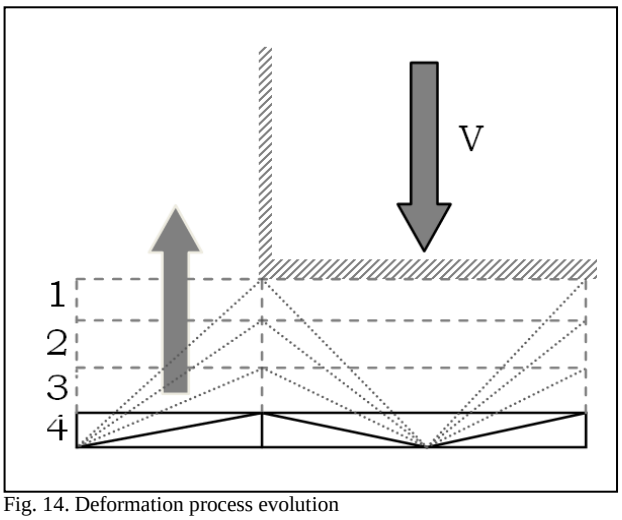

Fig. 14. Deformation process evolution

The Modular model begins to provide relatively higher data, in terms of Coulomb friction, when the model shape factor is equal or higher than 6 (*b/h* = 6). This is due to the extreme reduction of the modules, so the behavior of the graph can be explained by the accumulation of the material stress and hardering at that point of deformation, since the material would have a 70% reduction height. However, generally is not considered a bigger shape factor than 4 or 5.

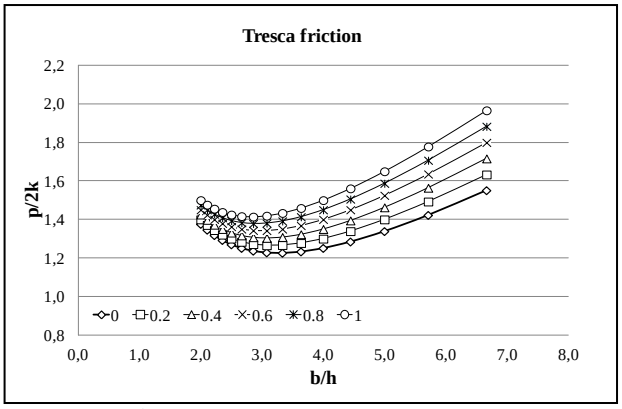

Fig. 15. Tresca friction p/2k variations

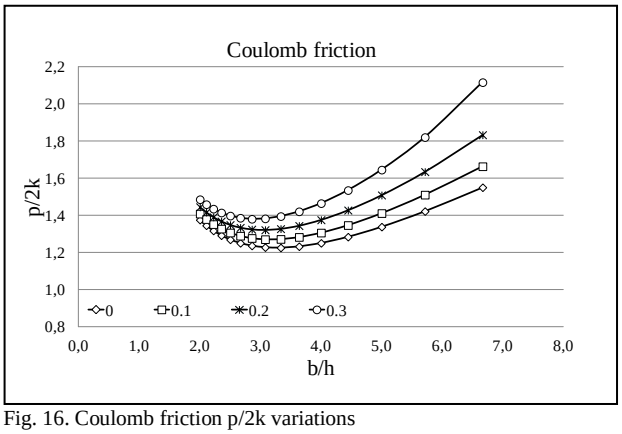

Fig. 16. Coulomb friction p/2k variations

At the graphs displayed in Fig. 15 and Fig. 16 shows the evolution of the *p/2k* ratio values through the results obtained as a function of the variation of the friction coefficient, Tresca and Coulomb friction, from its minimum to its maximum value, with similar behavior for all values of the range.

4. CONCLUSIONS

Concluded the model analysis and studied the influence of both type of friction for different shape factors, this work shows the advantage of lower computational cost offered by this method of calculation as well as having identified at any time the physical evolution of the problem.

The best configuration of modules is that one that determines the minimum value of required force to reach the desired state of deformation. Modular model is again the optimal solution for the present studies, because it satisfies the initial conditions of indentation, is fully consistent with the material deformation and achieves a much easier way to calculate and analyze the two types of friction considered.

Also, the Modulate alternative has a high versatility to adjust the Triangular Rigid Blocks disposition, obtaining an optimum adaptation to each of the geometries studied. This adaptation is performed by adding further modules, if necessary. In this case, unlike the Non Modular model, it doesn't complicate the equations, being similar to those that have been solved in the present work.

With the Non Modular model, equations become excessively complicated. If the study is a piece of larger dimensions, we would cope extremely complex equations because, as the numbers of modules are increasing, the equations are bigger and hence the resolution is often complex and cumbersome.

On the contrary, with the Modular model the resolution of the equations are easier owing the study is only of modules formed at most with three Triangular Rigid Blocks, so that the equations never become so complex, always being careful to drag previous speeds because, as explained above, the speed of next module input will be the output speed of the previous module.

5. FURTHER RESEARCH

Using the fundamentals of the UBT it is possible to improve the application of this method, by extending its analysis capability to more complex situations and providing more flexible results.

Thus, in this paper, the UBT using TRB has been applied to plane strain indentation processes but, in sake of completeness, the continuity of this work will be centered in the different configurations we can find of the punch, making the geometry as similar as industry procedures, studying in each case the friction present in the deformation process. It can be study an inclined flat dies. Due to this new point of view, the present work can be frame as a particular case in wich the inclination of the punch is 0º.

Further, working with friction, it can propound a combination of Tresca and Coulomb friction, being another approach to reality, as all plastic process undergoes to the two type of friction at the same time. And it would be a wider progress to asses the issue as though a case of not plane strain.

Thus all this work will give rise as a computer program that allows anyone to configure in an easy way, just with two or three parameters (base, high, punch type), a plastic deformation process and obtain the value of the minimum energy required to obtain such deformation process. Avoiding the others CAD and FEM programs, those requires many different parameters and, normally, are very difficult to use, e.g. the solutions given can rise to different interpretations that can lead, in turn, to numerous faults dragged by a bad approach or ignorance of any required parameter.

6. REFERENCES

[1] Chakrabarty J. (2006). *Theory of Plasticity*, Butterworth-Heinemann, ISBN 0-7506-6638, Oxford, UK

[2] Rubio E.M. (2012). Energetic analysis of tube drawing processes by the Upper Bound Method using the theoretical work-hardening materials, *Proceeding of Metal Forming 2012*, Kraków, Poland. In press

[3] Martín F.; Bermudo C. & Sevilla L. (2012). Analytical approach to the indentation process. Application of the Upper Bound Element Technique. *Material Science Forum*, Vol.713 pp. 13-18 ISSN: 0255-5476

[4] Li X. & Huang Y. (2012). Empirical models between user requeriments and product structural variables: A hydraulic forgind press case study. *Material Science Forum.* Vol. 697-698 pp.779-784, ISSN 0255-5476

[5] Rubio E.M.; Sebastián M.A. & Sanz A. (2003). Mechanical Solutions for drawing processes under plane strain conditions by the upper bound method. *J. Mat. Proc. Tech.* Vol. 143-144, pp.539-545, ISSN 0924-0136

[6] Huang M.; Tzou G & Fung R. (2007). Upper Bound solution to compression forming of three-layer bounded clad sheet. *Key Eng. Mat.* Vol. 340-341, pp.731-738, ISSN 1013-9826

[7] Martín F.; Sevilla L. & Sebastián M.A. (2009). Implementation of Technological and Geometrical Parameters in Forging Processes by Means of the Upper Bound Element Technique, AIP Conference Proceeding, Vol.1181(1), pp.455-463, ISSN 0094-243X, ISBN 978-0-7354-0722-0

[8] Hill R. (2004). *The Mathematical Theory of Plasticity* Oxford University Press Inc, New york, ISBN 0-19-850367-9

[9] Moon Y.H.; Van Tyne C.J. & Gordon W.A. (1995). The use of multiple flow for continuous solutions from Upper-Bound analysis, *Journal of Mat. Proc. Tech.* Vol. 52 pp. 561-596, ISSN 0924-0136

[10] Collins I.F. (1969). The Upper Bound Theorem for rigid/plastic solids generalized to include coulomb friction, *J. Mech. Phys. Solids*, Vol. 17, pp. 323-338, ISSN 0022-5096

[11] Bramley A. N. (2001). UBET and TEUBA: fast methods for forging simulation and preform design. *J. Mat. Proc. Tech.* Vol.116, pp. 62-66, ISSN 0924-0136

[12] Jun B. Y.; Kang S. M.; Lee M.C.; Park R. H. & Joun M. S. (2007). Prediction of geometric dimensions for cold forgings using the finite element method. *J. Mat. Proc. Tech.* Vol. 189 pp. 459-465, ISSN 0924-0136

[13] Wagoner, R.H. & Chenot, J.L. (2005). *Metal Forming Analysis*, Cambridge University Press, ISBN 9780-5-2101-7725, New York, USA

[14] Hsu, H. & Tzou, G. (2003). Two analytical models of double-layer clad sheet compresion forming based on the upper bound and the slab methods. *J. Mat. Proc. Tech.* Vol. 140 pp. 604-609, ISSN 0924-0136

[15] Martín F. (2009). Development, integration and optimization at the study of forging processes by the Upper Bound Theorem through Triangular Rigid Block model. Ph.D. Thesis, Department of Manufacturing Engineering, University of Malaga

[16] Rubio, E.M.; Camacho, A.M.; Marcos, M. & Sebastián, M.A. (2008). Analysis of the energy vanished by friction in tube drawing processes with a fixed conical inner plug by the upper bound method. *Materials and Manufacturing Processes*, Vol.23 (7), pp. 690-697, ISSN 1042-6914